Applied Catalysis A: General 462–463 (2013) 121–128

Contents lists available at SciVerse ScienceDirect

Applied Catalysis A: General

journal homepage: www.elsevier.com/locate/apcata

# Hydrogenation of 3-nitroacetophenone over rhodium/silica catalysts: Effect of metal dispersion and catalyst support

Majid I. Abdul-Wahab[1], S. David Jackson*

*Centre for Catalysis Research, WestCHEM, School of Chemistry, University of Glasgow, Glasgow G12 8QQ, Scotland, UK*

ARTICLE INFO

*Article history:*
Received 12 March 2013
Received in revised form 29 April 2013
Accepted 3 May 2013
Available online xxx

*Keywords:*
Hydrogenation
3-Nitroacetophenone
Rhodium/silica

ABSTRACT

The effect of physical properties of rhodium/silica catalysts on the hydrogenation of 3-nitroacetophenone was investigated using a series of catalysts with different particle sizes, pore sizes and dispersions. The hydrogenation reaction was carried out in the liquid phase at different temperatures (313–343 K) and hydrogen pressures (2–5 barg). The hydrogenation of 3-nitroacetophenone was found to be a consecutive reaction with 3-aminoacetophenone, 1-(3-aminophenyl) ethanol, and 1-(3-aminocyclohexyl) ethanol the main products; traces of 3-aminoaniline were also detected. The reaction was zero order with respect to the concentration of 3-nitroacetophenone and half order with respect to hydrogen. The rate of formation and disappearance of intermediates increased with increasing temperature and hydrogen pressure. The rate of ring hydrogenation to form 1-(3-aminocyclohexyl) ethanol shows a marked increase at high temperatures. The catalytic activity varies with both the pore size of silica support and the rhodium dispersion with no significant influence of catalyst particle size. The turnover frequency increases with decreasing metal dispersion (or with increasing average metal crystallite size) revealing an antipathetic particle size effect. This behaviour can be related to changes in the electronic and structural make up of small metal crystallites but suggests that the reaction takes place on the plane face surface of the FCC close-pack structure of rhodium in which the number of face surface atoms increases at the expense of the edge and corner sites as the metal crystallite size increases.



## 1. Introduction

The catalytic hydrogenation of 3-nitroacetophenone (3-NAP) to its corresponding products is an important reaction in the food and pharmaceutical industry. This hydrogenation process has not been the subject of significant study and is not covered well in the literature. The expected products mentioned in the available literature are 3-aminoacetophenone (3-AAP) and 1-(3-aminophenyl) ethanol (3-APE). 3-AAP is used as food flavouring and in synthesising pharmaceutical intermediates such as adrianol, and zaleplon [1]. 3-APE, is a useful intermediate in the synthesis of dyestuffs: it may be condensed with haloanthraquinones to yield arylaminoanthraquinones which, when devoid of water solubilising groups such as sulfo and carboxy, find utility in the field of polyester dyestuffs [2]. Early studies related to this reaction are to be found in the US patent literature namely, US patent 2,680,136 in 1954 [3], US patent 2,683,745 in 1954 [4], US patent 2,797,244 in 1957 [5], US patent 3,423,462 in 1969 [6], and US patent 4,021,487 in 1977 [2]. Most of these patents focused on the hydrogenation of 3-NAP to 3-AAP and sometimes to the alcohol, at relatively high pressures and temperatures using palladium or Raney nickel as catalysts. Hawkins et al. [7] studied the hydrogenation of 4-NAP to the corresponding amine, alcohol and ethyl aniline products via a parallel reaction screening using different palladium, platinum and rhodium catalysts. More recently, Jackson, et al. [1] has examined the hydrogenation of ortho, meta and para-nitroacetophenone to the respective aminoacetophenone in the liquid phase over a Pd/C catalyst. None of the previous work, to the best of our knowledge, gave the full profile of this reaction. In the present study, the hydrogenation of 3-NAP was investigated over six rhodium/silica catalysts different in their physical properties using a semi-batch reactor operated at different conditions of pressure, temperature, and catalyst loading. In the present hydrogenation process, 3-NAP was hydrogenated consecutively to 3-aminoacetophenone (3-AAP), 1-(3-aminophenyl) ethanol (3-APE), and 1-(3-cyclohexylamine) ethanol (3-ACHE), in addition to small amounts of 3-ethylaniline. In a subsequent paper a full kinetic analysis of the reaction sequence will be presented.

* Corresponding author. Tel.: +44 141 330 4443.
*E-mail address:* david.jackson@glasgow.ac.uk (S.D. Jackson).
[1] Present address: Chemical Engineering Department, University of Baghdad, Baghdad, Iraq.

0926-860X/$ – see front matter © 2013 Elsevier B.V. All rights reserved.
http://dx.doi.org/10.1016/j.apcata.2013.05.002

**Table 1**
Physical properties of Rh/silica catalysts.

| Catalyst code | Pore size (nm) | Particle size (μm) | Total pore length ($m\,g^{-1}$) | Surface area ($m^2\,g^{-1}$) | Average metal crystallite size (nm) | Rhodium dispersion (%) | Rhodium surface area ($m^2\,g^{-1}$) | Rhodium loading wt% | Pore volume ($ml\,g^{-1}$) |
|---|---|---|---|---|---|---|---|---|---|
| M01081 | 2.4 | 10.7 | 80,263 | 594 | 1.6 | 71 | 7.8 | 2.45 | 0.35 |
| M01272 | 6.4 | 10 | 24,308 | 488 | 1.8 | 60 | 6.6 | 2.30 | 0.78 |
| M01079 | 11.1 | 9.5 | 9814 | 344 | 1.2 | 94 | 10.3 | 2.29 | 0.96 |
| M01074 | 13.2 | 24 | 7740 | 321 | 2.6 | 43 | 4.7 | 2.50 | 1.06 |
| M01035 | 13.2 | 96.3 | 7740 | 321 | 3.5 | 32 | 3.5 | 2.20 | 1.06 |
| M01038 | 13.2 | 49.9 | 7740 | 321 | 2.7 | 41 | 4.5 | 2.20 | 1.06 |

## 2. Experimental

### 2.1. Catalysts

The catalysts used in the hydrogenation of 3-nitroacetophenone were rhodium catalysts supported on powder silica particles. Powder silica supports were supplied and characterised by Davison Catalysts. The active catalysts (Rh metal), which were supplied and characterised by Johnson Matthey, were prepared using an incipient-wetness method using aqueous rhodium chloride salts. Six catalysts, different in pore size, particle size, surface area, and metal crystallite size, were used to perform the hydrogenation reaction under different experimental conditions. Table 1 shows the physical properties of the as-supplied rhodium/silica catalysts [8].

### 2.2. Experimental setup

The hydrogenation reactions were performed using a 500 $cm^3$ capacity Buchi autoclave stirred tank reactor supplied with an oil heating jacket with a maximum operating temperature limit of 473 K. The temperature was measured in the liquid slurry with accuracy of ±1 K. The autoclave was designed to operate at a maximum operating pressure of 6 barg. The reactor was equipped with a variable speed stirrer connected to a magnetic drive. It was provided with gas inlet/outlet tubing for inert and hydrogen gas supply and gas venting. The reactor was connected to a Buchi press-flow gas controller to control the pressure of the reactor. The gas controller was used to measure the flow of hydrogen or inert gas to the reactor and also to measure the hydrogen gas consumed in the reaction. Fig. 1 shows the experimental reactor setup.

### 2.3. Experimental procedure

In a typical hydrogenation experiment, a known quantity of catalyst was charged with 300 ml of isopropyl alcohol (solvent) to the reactor and heated to the desired reduction temperature under slow stirring (300 rpm). An in situ reduction of the catalyst was performed by bubbling hydrogen gas at a flow rate of 280 $cm^3\,min^{-1}$ through this mixture for 30 minutes while stirring at 800 rpm. A measured quantity of 3-nitroacetophenone (Aldrich, 99%) was added to 25 ml of isopropyl alcohol in a conical flask and heated until all the 3-NAP was dissolved. After the reduction process was completed, the stirrer was turned off and the reactor was purged with nitrogen twice and pressurised to 1 barg pressure. The contents were then heated to the desired reaction temperature under slow stirring. After reaching the desired temperature, the stirrer was turned off and the 3-NAP solution was added to the reactor vessel through the reactor inlet, which was then flushed with 25 ml of isopropyl alcohol to give a total reaction volume of 350 ml. The solution was stirred at 800 rpm for 5 s to allow mixing. The stirrer was then turned off and the reactor pressurised with $N_2$ to 1 barg. A sample of 2.5 ml was withdrawn. The reactor was de-pressurised, before being purged twice with hydrogen then pressurised with hydrogen to the desired reaction pressure. Once the vessel was pressurised the reaction was started by switching the stirrer on at 1000 rpm: this was taken as the zero time of the reaction. The progress of the reaction was followed by withdrawing samples of 2.5 ml at different time intervals along the reaction period of 6 h. The moles of hydrogen consumed during the reaction were also monitored and recorded. The liquid samples were analysed using a Thermo Finnigan Focus GC equipped with an AS 3000 autosampler. The column was HP-1701, 30 m × 0.25 mm × 1 μm film thickness. FID temperature was 523 K, injector temperature was 503 K, and the column temperature was fixed at 433 K. The hydrogenation experiments were performed at 3-NAP initial concentrations of 0.0075, 0.015, and 0.0225 $mol\,l^{-1}$, temperatures of 313, 323, 333, and 343 K, hydrogen pressures of 2, 3, 4, and 5 barg, and catalyst weights of 0.05 and 0.1 g. The conversion of 3-nitroacetophenone and the yields of 3-aminoacetophenone (3-AAP), 1-(3-aminophenyl) ethanol (3-APE), and 1-(3-aminocyclohexyl) ethanol (3-ACHE) were calculated using the following correlations:

$$X_{3-\mathrm{NAP}} = \frac{[3-\mathrm{NAP}]_o - [3-\mathrm{NAP}]_t}{[3-\mathrm{NAP}]_o} \times 100 \quad (1)$$

$$Y_{3-\mathrm{AAP}} = \frac{[3-\mathrm{AAP}]_t}{[3-\mathrm{NAP}]_o} \times 100 \quad (2)$$

$$Y_{3-\mathrm{APE}} = \frac{[3\mathrm{APE}]_t}{[3-\mathrm{NAP}]_o} \times 100 \quad (3)$$

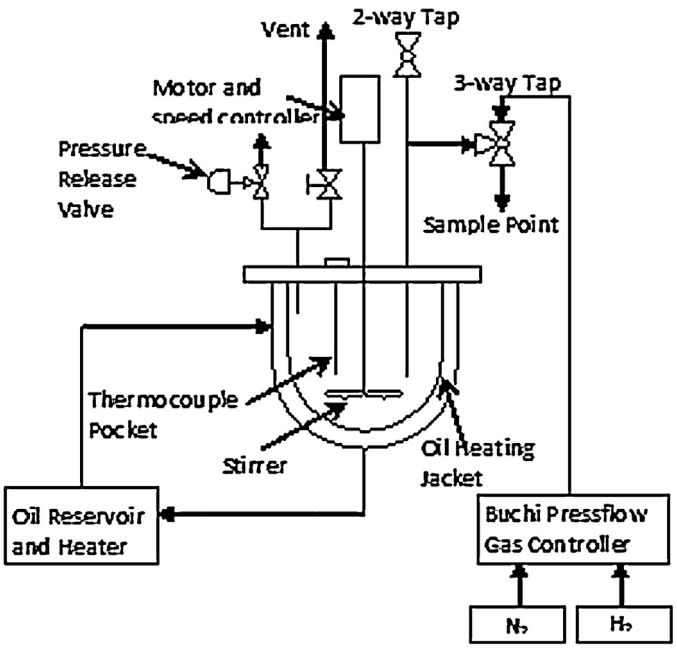


**Fig. 1.** Schematic diagram of the experimental setup.

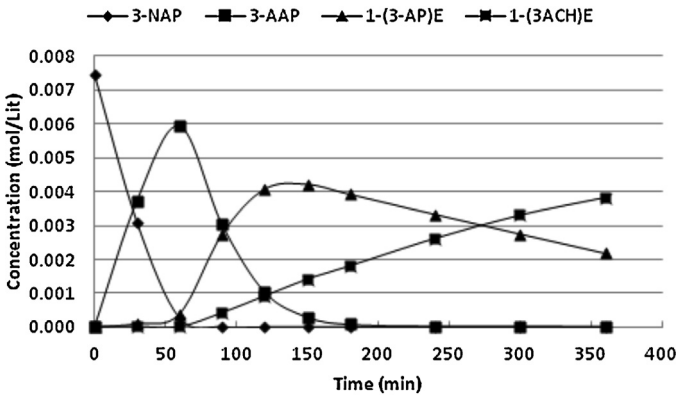


**Fig. 2.** Typical concentration–time profiles for hydrogenation of 3-NAP using $Rh/SiO_2$ (M01079) catalyst. Reaction conditions: catalyst weight = 0.05 g; temperature = 333 K; $H_2$ pressure = 4 barg.

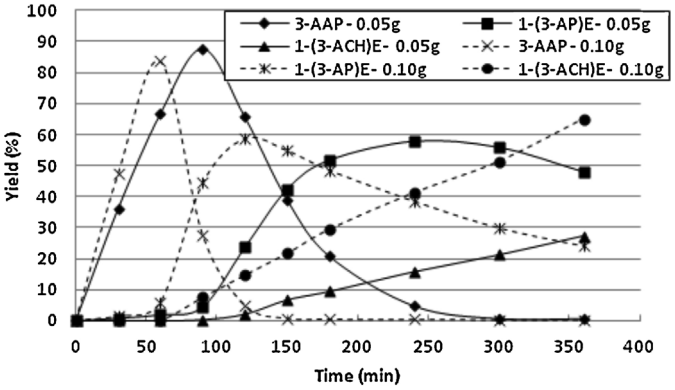


**Fig. 4.** Yields of reaction products with time for different catalyst weights. reaction conditions: catalyst, M01079; temperature = 333 K; $H_2$ pressure = 4 barg.

$$Y_{3-\mathrm{ACHE}} = \frac{[3\mathrm{ACHE}]_t}{[3-\mathrm{NAP}]_o} \times 100 \quad (4)$$

where, $X$ is the conversion, $Y$ is the yield, $[3\text{-NAP}]_o$ is the initial concentration of 3-NAP, $[3\text{-NAP}]_t$, $[3\text{-AAP}]_t$, $[3\text{-APE}]_t$, and $[3\text{-ACHE}]_t$, are the concentrations of 3-NAP, 3-AAP, 3-APE, and 3-ACHE respectively at any time.

## 3. Results

In the present study, hydrogenation of 3-nitroacetophenone took place through a series of consecutive reactions. Preliminary experiments were performed to study the product distribution and selectivity behaviour using the $Rh/SiO_2$ catalysts. The effect of catalyst particle size, metal crystallite size, and pore size was investigated for a range of $Rh/SiO_2$ catalysts at different temperature, hydrogen pressure and catalyst loading conditions.

### 3.1. Reaction products distribution

Both the choice of catalyst and the reaction parameters have significant effects on the yields of the hydrogenation products. A typical concentration–time profile of various components involved in the hydrogenation of 3-NAP using $Rh/SiO_2$ is shown in Fig. 2. It was observed that 3-NAP underwent hydrogenation of the $-NO_2$ group to form 3-aminoacetophenone.

The concentration of the 3-aminoacetophenone rose to a maximum before it fell when hydrogenated further to 1-(3-aminophenyl) ethanol, which in turn was hydrogenated via ring hydrogenation to 1-(3-aminocyclohexyl) ethanol. The GC analysis also detected trace levels of 3-ethyl aniline (<1%). These reaction species accounted for about 90–95% of the material balance. The hydrogenation of 3-AAP to subsequent products was limited until the conversion of 3-NAP was nearly completed. Similarly, the conversion of 3-APE to 3-ACHE took place only after 3-AAP concentrations became very small. Based on the products identified by GC analysis, the reaction scheme is shown in Fig. 3.

The yields of 3-AAP, 3-APE, and 3-ACHE varied with the variation of the reaction conditions and catalyst loading. Fig. 4 shows the variation of the yields with the catalyst loading at certain reaction conditions. It can be noticed that doubling the catalyst weight from 50 mg to 100 mg nearly doubles the rate of reaction for the same reaction conditions, indicating the absence of mass transfer effects in this catalyst. The yields of 3-AAP are shown in Fig. 5 for all the catalysts studied. All the catalysts have a nearly identical percentage of active metal, however as can be seen, the rate of formation and disappearance of 3-AAP differs on each catalyst. Generally, the rates were higher over catalysts M01038, M01035, and M01074, which have the largest pore sizes (13.2 nm), compared to the other catalysts while the slowest rate was observed with catalyst M01081, which has the smallest pore size (2.4 nm). Fig. 6 shows the yield of 3-APE for all the catalysts studied. Again the rates of formation and consumption of 3-APE were higher in

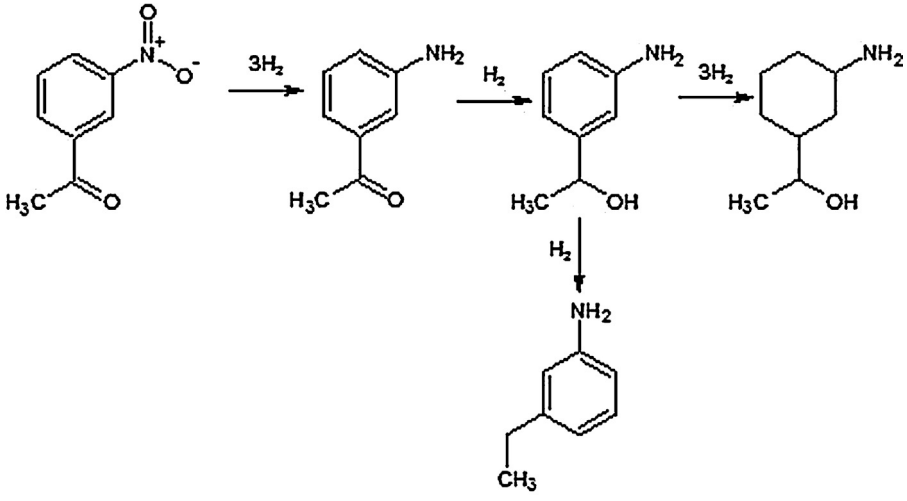


**Fig. 3.** Reaction scheme for hydrogenation of 3-NAP over $Rh/SiO_2$.

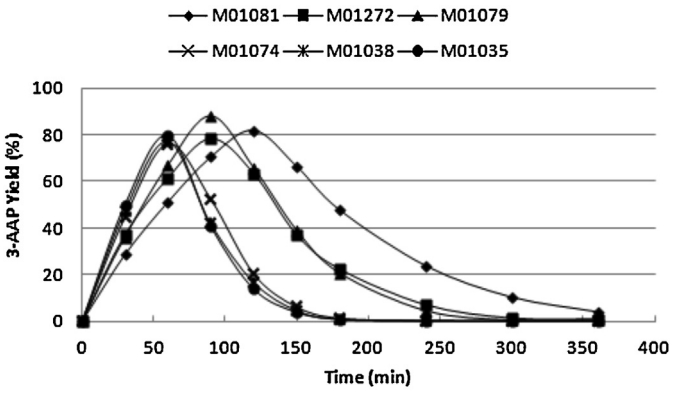


**Fig. 5.** Yields of 3-aminoacetophenone for different catalysts. Reaction conditions: catalyst weight = 0.05 g; temperature = 333 K, $H_2$ pressure = 4 barg.

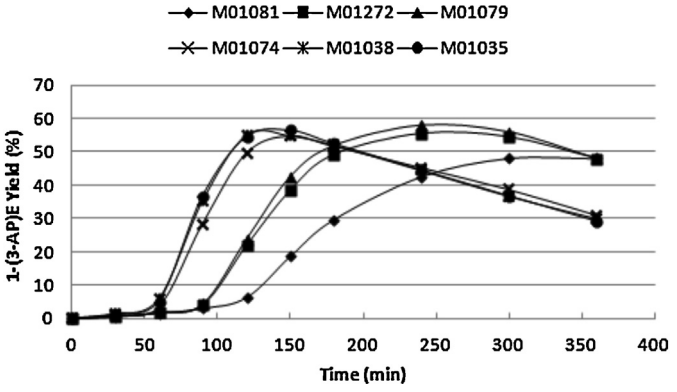


**Fig. 6.** Yields of 1-(3-aminophenyl) ethanol for different catalysts. Reaction conditions: catalyst weight = 0.05 g; temperature = 333 K, $H_2$ pressure = 4 barg.

the case of catalysts M01038, M01035, and M01074, compared to other catalysts. These catalysts also showed a larger tendency for ring hydrogenation to 3-ACHE. Catalyst M01081, of course, is the slowest in producing 3-aminophenyl ethanol and also in the ring hydrogenation. The same trend was noticed for the production of 1-(3-aminocyclohexyl) ethanol (Fig. 7).

### 3.2. Effects of mass transfer

In order to examine the effect of mass transfer on the hydrogenation reaction, a series of tests were performed to ensure that there was no mass transfer resistance interference with the intrinsic rate measurements. To investigate whether film mass transfer

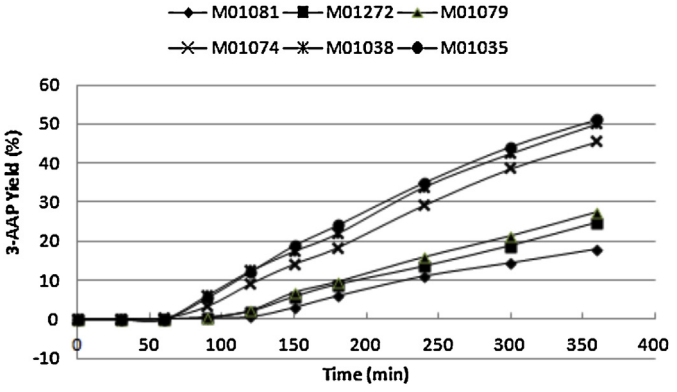


**Fig. 7.** Yields of 1-(3-aminocyclohexyl) ethanol for different catalysts. Reaction conditions: catalyst weight = 0.05 g; temperature = 333 K, $H_2$ pressure = 4 barg.

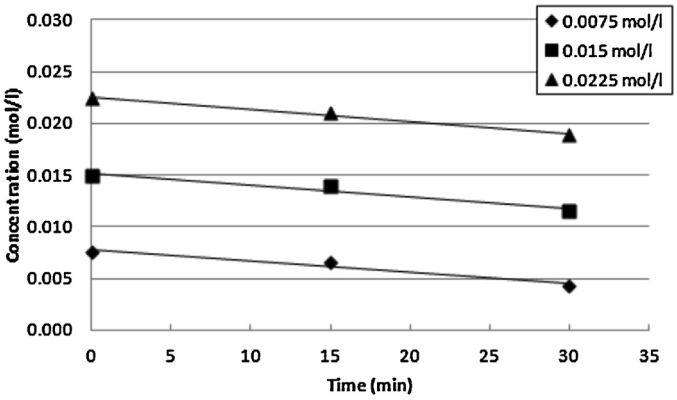


**Fig. 8.** Concentration–time profiles for hydrogenation of 3-NAP using different 3-NAP initial concentrations. Reaction conditions: catalyst weight (M01079) = 0.05 g; temperature = 333 K; $H_2$ pressure = 3 barg.

has an effect on the reaction rate, four experiments were carried out with different stirrer speeds (600, 800, 1000 and 1200 rpm) while all other reaction conditions were held constant. Hydrogen consumption was almost identical in all tests indicating that gas-film mass transfer had no significant effect on the rate of reaction. Liquid–solid mass transfer limitations were tested by doubling the catalyst weight for the same reaction conditions. The results show that doubling the catalyst amount approximately doubles the rate of reaction, which indicates the absence of liquid–solid mass transfer effects. Pore diffusion, in general, is not likely to take place in liquid phase reactions because pore diffusion (mainly Knudsen diffusion) normally relates to gases rather than liquids since the mean free path for molecules of liquid is very small and may be close to the diameter of the molecule itself [9]. In the present study, the lowest pore size was in catalyst M01081 (2.4 nm), which is approximately 8 times the molecular diameter (0.309 nm) of 3-NAP. However, this catalyst showed less activity for the hydrogenation reaction when compared to the other catalysts, which indicate the possibility of a mass transfer contribution in the kinetics of the reaction.

### 3.3. Effect of 3-NAP initial concentration

In order to investigate the effect of the initial concentration of 3-NAP on the rate of reaction, the hydrogenation was carried out using 3-NAP with initial concentrations of 0.0075, 0.015, and 0.0225 mol $l^{-1}$. Fig. 8 shows the concentration–time profiles of 3-NAP using catalyst M01079, with all other reaction conditions kept constant. One must be careful in calculating the reaction rate when using different concentrations, as the instantaneous rates will differ as the reaction proceeds. Therefore, the initial rate over a short period of time must be calculated. The hydrogen consumption profile indicates that $H_2$ uptake was nearly the same for the first 15 minutes of the reaction times. The rates were approximately identical for the three initial concentrations at $1.08 \times 10^{-4}$, $1.15 \times 10^{-4}$, and $1.17 \times 10^{-4}$ mol $l^{-1}$ $min^{-1}$, indicating that the initial concentration of 3-NAP has a negligible effect on the rate of reaction and the hydrogenation reaction can be considered as zero order with respect to 3-NAP concentration.

### 3.4. Effect of temperature and hydrogen pressure

Hydrogenation of 3-NAP was carried out at different temperatures, 313, 323, 333, and 343 K and different hydrogen pressures, 2, 3, 4, and 5 barg. A significant enhancement in the activity was observed with the increase in the reaction temperature (Fig. 9). The complete conversion of 3-nitroacetophenone was reached after 300 min at 313 K, while it was reached after 60 min at 343 K for the

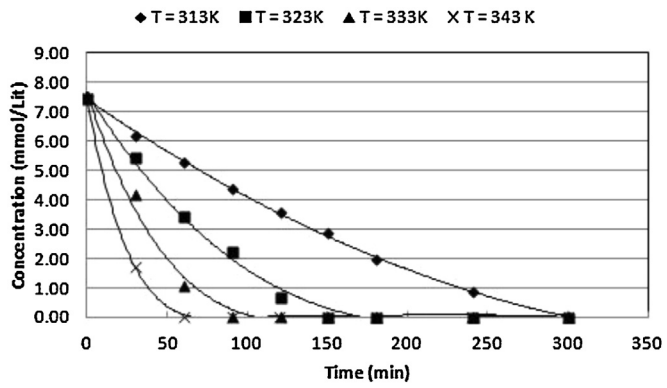


**Fig. 9.** Concentration profiles of 3-NAP at different temperatures using catalyst M01079. Reaction conditions: catalyst weight = 0.05 g; $H_2$ pressure = 4 barg.

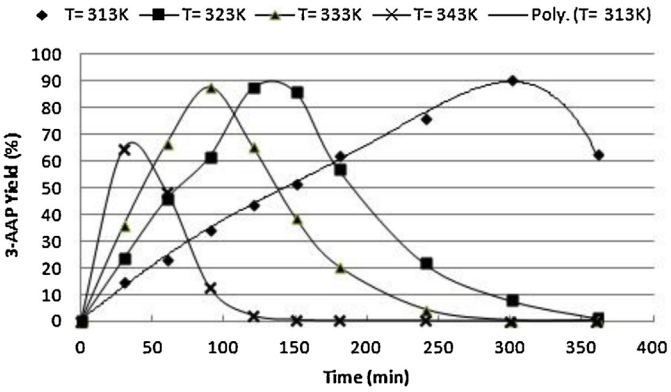


**Fig. 10.** Yields of 3-AAP at different temperatures using catalyst M01079. Reaction conditions: catalyst weight = 0.05 g; $H_2$ pressure = 4 barg.

catalyst M01079. The effect of temperature on the product yields is shown in Figs. 10–12. The yield of 3-AAP decreased as the reaction temperature increased from 313 to 343 K due to the formation of the alcohol. The behaviour of 3-APE was similar as its concentration rose and then fell as 3-ACHE was formed. The drop in concentration was more rapid with the increase in reaction temperature. The ring hydrogenation of 1-(3-aminophenol) ethanol was relatively slow at low temperatures but became faster at higher temperatures indicating that if it is desired to have high selectivity of 3-APE, the reaction should be carried out at low temperatures (less than 323 K). Arrhenius plots of the hydrogenation of 3-NAP to 3-AAP with varying reaction temperatures (313, 323, 333, and 343 K)

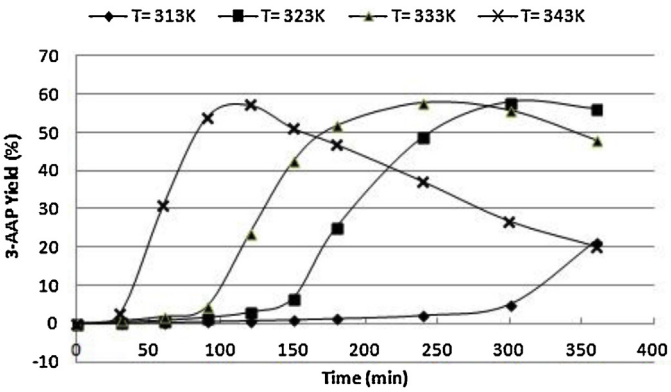


**Fig. 11.** Yields of 3-APE at different temperatures using catalyst M01079. Reaction conditions: catalyst weight = 0.05 g; $H_2$ pressure = 4 barg.

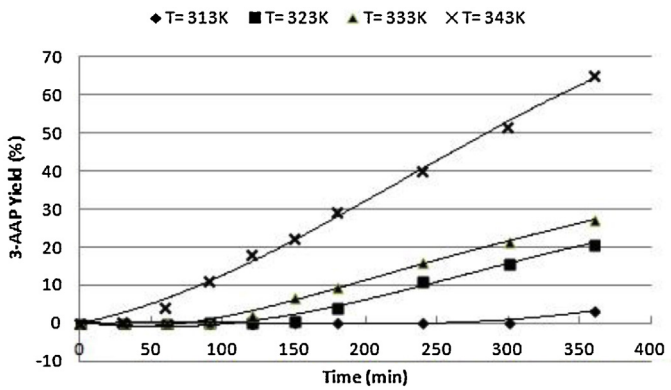


**Fig. 12.** Yields of 3-ACHE at different temperatures using catalyst M01079. Reaction conditions: catalyst weight = 0.05 g; $H_2$ pressure = 4 barg.

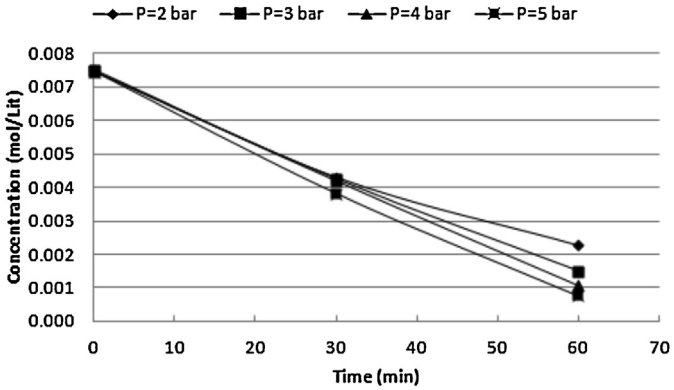


**Fig. 13.** Concentration of 3-NAP for different hydrogen pressure using catalyst M01079. Reaction conditions: catalyst weight = 0.05 g; temperature = 333 K.

were used to estimate the apparent activation energies for all the catalysts used. Table 2 shows that rhodium/silica catalysts with different physical properties have different activation energies for the hydrogenation reaction.

The effect of hydrogen pressure was tested by carrying out experiments at different hydrogen pressures (2, 3, 4, and 5 barg) to examine the effect of the change in pressure on the rate of the hydrogenation reaction. Fig. 13 shows that the hydrogen pressure influenced the rate of 3-NAP hydrogenation. Table 3 shows the order of reaction with respect to the change of hydrogen pressure for all the catalyst used. The orders lies in the range of 0.4–0.5 for

**Table 2**
Activation energies for the hydrogenation of 3-NAP.

| Catalyst | Activation energy (kJ $mol^{-1}$) |
|---|---|
| M01081 | 68.4 |
| M01272 | 47.3 |
| M01079 | 43.9 |
| M01074 | 40.0 |
| M01038 | 57.6 |
| M01035 | 43.4 |

**Table 3**
Reaction order with respect to hydrogen pressure.

| Catalyst | Reaction order |
|---|---|
| M01081 | 1.3 |
| M01272 | 0.4 |
| M01079 | 0.4 |
| M01074 | 0.4 |
| M01038 | 0.5 |
| M01035 | 0.4 |

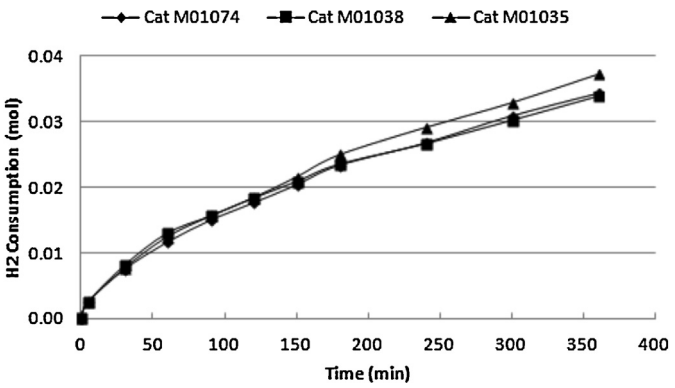


**Fig. 14.** Hydrogen consumptions for catalysts with different particle sizes. Reaction conditions: catalyst loading = 0.05 g; temperature = 333 K; $H_2$ pressure = 4 barg.

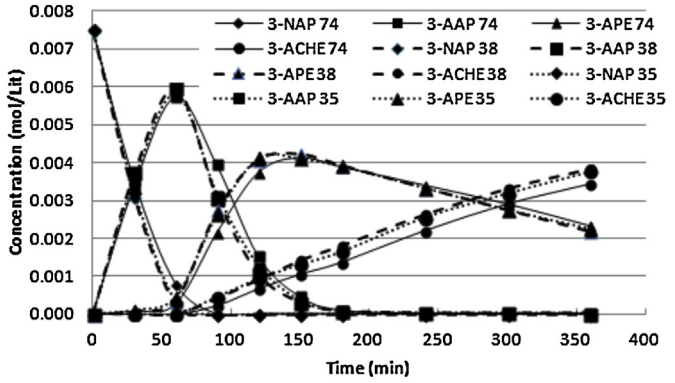


**Fig. 15.** Concentration–time profiles for hydrogenation of 3-NAP using $Rh/SiO_2$, for catalysts M01074, M01038, and M01035. Reaction conditions: catalyst weight = 0.05 g; temperature = 333 K; $H_2$ pressure = 4 barg.

all the catalysts except for catalyst M01081, which has the lowest pore size (2.4 nm) and had an order of 1.3.

### 3.5. Effect of catalyst particle size

Three of the $Rh/SiO_2$ catalysts; M01074, M01038, and M01035 were tested for the effect of particle size on the rate of hydrogenation reaction. These catalysts have identical pore sizes (13.2 nm) and surface area (321 $m^2\,g^{-1}$) but different particle sizes (24, 49.9, and 96.6 μm respectively). Fig. 14 shows the hydrogen consumption curve and Table 4 shows the initial rate of the reaction. It can be observed that the difference in particle sizes of the catalysts had only a minor effect on the initial rate of the hydrogenation reaction. Although the reaction profiles were similar for all the reactions performed (Fig. 15), there was a slight increase in the initial rate when going from catalyst M01074 (particle size = 24 μm) to M01038 (particle size = 96.6 μm). The yield of 3-AAP with conversion shows a minor effect of particle size on the yield even for different temperatures.

**Table 4**
Initial reaction rate for $Rh/SiO_2$ catalysts of different particle sizes.

| Catalyst | Cat M01074 PS = 24 μm | Cat M01038 PS = 49.9 μm | Cat M01035 PS = 96.6 μm |
|---|---|---|---|
| Initial rate (mmol $min^{-1}\,g^{-1}$) | 5.25 | 5.62 | 5.52 |

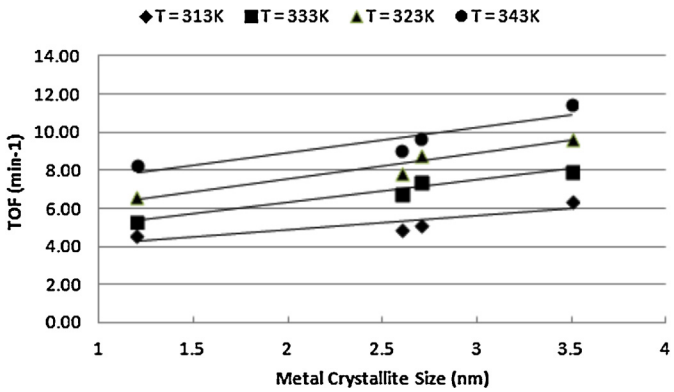


**Fig. 16.** Turnover frequency versus metal crystallite size at different reaction temperatures. Reaction conditions: catalyst weight = 0.05 g; $H_2$ pressure = 4 barg.

### 3.6. Effect of catalyst metal crystallite size

Metal crystallite size is normally used as a measure of metal dispersion on the silica support. Metal dispersion was calculated as the ratio of the moles of surface metal to the total moles of metal (Eq. (5)).

$$\text{Dispersion}\% = \frac{SA_{Rh}Mwt}{A_{Rh}NW_{Rh}} \times 100 \quad (5)$$

where $SA_{Rh}$ is the metal surface area per unit catalyst weight ($m^2\,g^{-1}$), $A_{Rh}$ is the area of Rh atom ($m^2$) which is taken as $7.52 \times 10^{-2}\,m^2$ [8], $N$ is Avogadro number ($6.02 \times 10^{23}$), and $W_{Rh}$ is the percentage of the catalyst metal loading. Table 1 shows the percentage dispersion of the various rhodium catalysts. The hydrogenation activity of the catalysts was compared using the turnover frequency rather than the reaction rate because the catalysts had different metal surface areas. TOF is defined as the number of molecules of hydrogen consumed per surface Rh atom per minute. It is calculated by using the following equation:

$$\text{TOF} = \frac{n_{H_2}\text{reacted}}{n_{Rh}} \quad (6)$$

where $n_{H2\ reacted}$ is the number of moles of hydrogen reacted per minute per gram of catalyst and $n_{Rh}$ is the number of moles of surface rhodium per gram of catalyst. Catalysts, M01074, M01038, and M01035, which have identical surface area and pore diameters but differ in metal crystallite size and catalyst M01079 which differs slightly in pore size (Table 1), were used to investigate the effect of metal crystallite size (or metal dispersion) on the activity of the catalysts. A plot of TOF vs. metal crystallite size at different reaction temperatures is shown in Fig. 16. There is an obvious increase in TOF with the metal crystallite size of the catalysts which becomes steeper with increasing temperature.

### 3.7. Effect of catalyst pore size

Catalysts M01081, M01272, and M01079 were used to investigate the effect of the pore size on the activity of the catalysts in the hydrogenation reaction. To decouple the effect of differences in average metal crystallite sizes of the above catalysts, the method applied by Hindle et al. [8] in which the metal crystallite size was normalised to 1 nm was adopted. Fig. 17 shows a plot of TOF values versus pore size at different reaction temperatures. As expected, catalyst M01081, which had the smallest pore size (2.4 nm) gave the smallest TOF value compared to the other catalysts, which gave nearly identical values. It can be concluded that the pore size has a significant effect on the catalyst M01081 and only minor effects on the other two catalysts. The effect of temperature on the catalyst

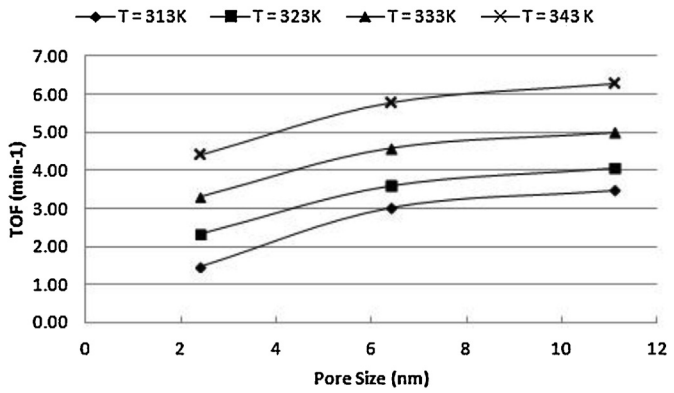


**Fig. 17.** Turnover frequency versus catalyst pore size at different reaction temperatures. Reaction conditions: catalyst weight = 0.05 g; $H_2$ pressure = 4 barg.

activity is clear as TOF increases with increasing of reaction temperature; however, the rate of increase of TOF becomes larger at the higher temperatures.

## 4. Discussion

The aim of the present work was to study the hydrogenation of 3-nitroacetophenone and more particularly, the production of 3-aminoacetophenone, 1-(3-aminophenyl) ethanol and 1-(3-aminocyclohexyl) ethanol by the catalytic hydrogenation of 3-nitroacetophenone using different rhodium/silica catalysts in a semi-batch reactor at different reaction conditions. 3-NAP hydrogenation is a complex multi-step reaction due to competitive hydrogenation between nitro, carbonyl, and phenyl groups in one molecule. Prior to discussing the results, it is important to note that there is no significant information about the mechanism of hydrogenation of 3-nitroacetophenone in the literature. Therefore, some analogous reactions are examined to reveal useful information regarding the formation of products.

In the previous studies of hydrogenation of 3-nitroacetophenone [1–3,5] and other studies on the hydrogenation of compounds containing nitro group such as nitrobenzene [1,10–13], hydrogenation of the nitro group is expected to occur faster than other functional groups, due to the strong electronegativity of the nitro group, which comes from the combined action of the two electron-deficient oxygen atoms bonded to the partially positive nitrogen atom; hence 3-aminoacetophenone was expected, and found, as the first main product. The hydrogenation of 3-AAP is more complex due to the competitive hydrogenation between phenyl and carbonyl groups. Hydrogenation of acetophenone [14], in the absence of the amine functionality, showed different possible products depending on the catalysts used, for example products detected over a Pd-based catalyst [15] were 1-phenylethanol and ethylbenzene, while over a Pt-based catalyst 1-phenylethanol, ethylbenzene, methylcyclohexylketone, cyclohexylethanol and ethylcyclohexane were all observed [16]. Examination of the present experimental results shows that the hydrogenation of the carbonyl group in 3-AAP has priority over hydrogenation of the phenyl group over silica supported Rh catalysts. The ring hydrogenation of 3-AAP did not take place during the reaction, since there was no 1-methyl-(3-aminocyclohexyl) ketone detected in the products. Therefore, Rh catalysts can be considered as good catalysts for the selective hydrogenation of the carbonyl group. The concentration of 3-aminoacetophenone increases to a maximum value and then decreases with reaction time, as the concentration of 1-(3-aminophenyl) ethanol increases and then decreases, while finally the concentration of 1-(3-aminocyclohexyl) ethanol slowly grows with time. This means that the formation of 3-AAP, 3-APE, and 3-ACHE is consecutive reactions. No useful literature was found concerning the formation of 1-(3-aminocyclohexyl) ethanol by ring hydrogenation of 1-(3-aminophenyl) ethanol. When the concentration of 3-APE became large enough, especially at high temperatures, a small amount of 3-ethylaniline (<1%) was produced. This is could be due to the dehydration reaction of 1-(3-aminophenyl) ethanol to give 3-aminostyrene, which would then be rapidly transformed to 3-ethylaniline by hydrogenation. However no 3-aminostyrene was observed and the reaction may be direct reduction of the alcohol.

The rate of the hydrogenation reactions was affected by the physical characteristics of catalysts and the operating conditions such as temperature and pressure. Results show that increasing the initial concentration of 3-NAP from 0.0075 to 0.0225 mol $l^{-1}$ did not alter the initial rate of the reaction. Therefore, the hydrogenation reaction order with respect to 3-NAP concentration is zero order. Hydrogen pressure has also a significant effect on the rate of the reaction and the yields. The initial rate of 3-NAP hydrogenation increased with an increase of the initial hydrogen pressure in the reactor. This result agrees with many previous studies on the hydrogenation of aromatic nitro species [1,10–12]. With most of the catalysts the reaction order in hydrogen is ~0.5 (Table 3). Such a value is consistent with a Langmuir–Hinshelwood description of the reaction kinetics with hydrogen being dissociated and weakly adsorbed relative to the 3-NAP. The single catalyst, which gives a different value for the reaction order in hydrogen, is M01081 with a value that approximates to first order. This catalyst has the smallest pore size and, as will discussed later, shows mass transfer control effects in the hydrogenation. Typically mass transfer controlled reactions exhibit first order kinetics; hence the value of ~1 for the reaction order with respect to hydrogen pressure is not surprising. Therefore for this catalyst, only kinetic terms modified by mass transfer control will be observed. Changing the temperature of the reaction allowed a determination of the activation energy for the hydrogenation of the 3-NAP to 3-AAP (Table 2). The value that is significantly different from the rest is that of catalyst M01081. It would be expected that the effect of mass transfer control on the reaction would lower the observed activation energy to a value $\leq$20 kJ $mol^{-1}$, however the reverse is found with an observed activation energy of ~68 kJ $mol^{-1}$. This behaviour may be related to the exothermic nature of the reaction, which can result in a temperature difference between the bulk and the surface of the catalyst particle leading to an enhanced value for the apparent activation energy [17].

The investigation of the effect of average metal crystallite size or metal dispersion on the turnover frequency, which showed that the turnover frequency decreased with an increase in rhodium dispersion, is consistent with previously reported observations, for example, platinum supported catalysts showed that the turnover frequency increased with a decrease in platinum dispersion along with an increase in the acidity of support materials [18]. Hydrogenation of para-toluidine on $Rh/SiO_2$ catalysts also displayed a decrease in catalyst activity with the increase in metal dispersion [19]. The antipathetic relationship between metal dispersion and TOF can be attributed to the nature of the rhodium metal crystals and the specificity of the reaction site. The structure of rhodium crystals is of face-centred cubic (FCC), which is a close-pack structure with atomic packing factor (APF) of 0.74. When the metal crystal size increases, the number of face surface atoms increases at the expense of the edge and corner sites of the structure. The increase of turnover frequency with the increase of the metal particle size suggests that the hydrogenation reaction takes place on the plane face surface as opposed to edge and corner sites. Matsuhashi et al. [20] in their comprehensive study on the effect of metal dispersion in many catalytic reactions over platinum catalysts concluded that the relation between the TOF and

platinum dispersion was negative in a number of reactions such as, combustion of propane, oxidation of CO, hydrogenations of ethylene and naphthalene, hydrodechlorination of trichloroethane and hydrodesulfurization of thiophene. They indicated that the activity increases with decreasing metal particle size when the active sites exist on the edges or corners of metal surfaces, which increases with increasing dispersion. Our interpretation of the results from the present study is in keeping with this conclusion. Nevertheless care must be taken as this explanation has in-built assumptions such as the need for the metal crystallites to have complete outer layer. Many crystallites will have defects and will not have complete crystal structures. Another property that changes with metal crystallite size is the electronic structure of the metal. In a recent publication [21] it has been proposed that below 10 nm it is the electronic factor that will have the largest effect on a surface sensitive reaction rather than the geometric factor and in our study all the catalysts have average metal crystallite sizes well below 10 nm. Indeed in small metal crystallites geometric and electronic factors are inextricably linked and both will play a role in structure sensitivity of small metal crystallites [21–24].

Although the liquid–solid reaction systems can usually be considered safe from pore diffusion effects, the results show that catalyst M01081with the smallest pore size (2.4 nm) has the lowest activity among the catalysts studied, which may indicate the existence of some diffusion resistance within this catalyst. The result of the variation of TOF with pore size, shown in Fig. 17, confirms this interpretation. Other catalysts which have pores sizes of 6.4, 11.1, and 13.2 nm show nearly identical TOF values. Therefore, it can be concluded that the pore diffusion can be avoided in the hydrogenation of 3-NAP, when using $Rh/SiO_2$ catalysts with pore sizes larger than 6.4 nm.

## 5. Conclusion

Silica-supported rhodium catalysts were used in the investigation of the effects of catalyst physical properties and reaction conditions on the hydrogenation of 3-nitroacetophenone. The results show that the reaction is consecutive with 3-aminoacetophenone, 1-(3aminophenyl) ethanol, and 1-(3-aminocyclohexyl) ethanol the major products. The reactivity of the functional groups to hydrogenation over $Rh/SiO_2$ catalysts is nitro > carbonyl > phenyl. The initial hydrogenation reaction is zero order with respect to 3-nitroacetophenone concentrations and half order (0.5) with respect to hydrogen. The rate of reaction increases with increasing temperature resulting in activation energies between 40 and 60 kJ $mol^{-1}$. The rate of formation and consumption of intermediates varies with temperature and hydrogen pressure. A full kinetic analysis of the sequential reactions will be published in a subsequent paper. The yield of the final product, 1-(3-aminocyclohexyl) ethanol, shows a marked increase at high temperatures (more than 333 K). The results show that the physical properties of the catalyst support have significant effect on the activity of the catalyst. The effects of dispersion, particle size and pore size of catalysts have been presented. It is observed that with the catalyst particle size range used in the present study (9.5–96.3 μm), the size of catalyst particles has only minor effect on the activity. The pore size of the catalyst support however has a marked effect on TOF for the catalyst of pore size less than 6.4 nm while the catalysts with pore sizes larger than 6.4 nm show nearly identical TOF values. The metal dispersion shows an antipathetic relationship with the activity of the catalyst, such that catalysts with higher dispersion values or smaller metal crystallite sizes show lower TOF values. This behaviour can be related to changes in the electronic and structural make up of small metal crystallites and may indicate that the reaction takes place on the faces of the FCC rhodium close-pack crystalline structures.

## Acknowledgments

Financial support from the Institute of International Education (IIE) and SRF Iraq-Project are gratefully acknowledged.

## References

[1] S.D. Jackson, R. McEwan, R.R. Spence, in: M.J. Prunier (Ed.), Catalysis of Organic Reactions, 22nd Conference, CRC Press, Boca Raton, 2008, pp. 79–86.
[2] W. Michalowicz, L. Haven, U.S Patent 4021487, 1977.
[3] J. Lomartire, N.J. Summit, US Patent 2,680,136, 1954.
[4] W. Emerson, R.A. Helmsch, U.S Patent 2,683,745, 1954.
[5] S.W. Tinsley, S. Charleston, U.S. Patent 2,797,244, 1957.
[6] P.N. Rylander, U.S. Patent 3,423,462, 1969.
[7] J.M. Hawkins, T.W. Makowski, Org. Process Res. Dev. 5 (2001) 328–330.
[8] K.T. Hindle, S.D. Jackson, D. Stirling, G. Webb, J. Catal. 241 (2006) 417–425.
[9] O. Levenspiel, Chemical Reaction Engineering, 3rd ed., Wiley, New York, 1999, pp. 378.
[10] E.A. Gelder, University of Glasgow, 2005, PhD Thesis.
[11] E.A. Gelder, S.D. Jackson, C.M. Lok, Catal. Lett. 84 (3/4) (2002) 205–208.
[12] C. Li, Y. Chen, W. Wang, Appl. Catal. A 119 (1994) 185–194.
[13] P. Sangeetha, K. Shanthi, K.S. Rama Rao, B. Viswanathan, P. Selvam, Appl. Catal. A 353 (2009) 160–165.
[14] X.B. Zhang, React. Kinet. Mech. Catal. 102 (2011) 417–421.
[15] C. Chen, H. Chen, Appl. Catal. A 260 (2004) 207–213.
[16] C. Chen, H. Chen, W. Cheng, Appl. Catal. A 248 (2003) 117–128.
[17] M.E. Davis, R.J. Davis, Fundamentals of Chemical Reaction Engineering, McGraw-Hill Co., New York, 2003, pp. 184.
[18] Y. Yazawa, H. Yoshida, T. Hattori, Appl. Catal. A 237 (2002) 139–148.
[19] K.T. Hindle, S.D. Jackson, G. Webb, in: J.R. Sowa Jr. (Ed.), Catalysis of Organic Reactions, 20th Conference, CRC Press, Boca Raton, 2005, pp. 77–84.
[20] H. Matsuhashi, S. Nishiyama, H. Miura, K. Eguchi, K. Hasegawa, Y. Iizuka, A. Igarashi, N. Katada, J. Kobayashi, T. Kubota, T. Mori, K. Nakai, N. Okazakim, M. Sugioka, T. Umekio, Y. Yazawa, D. Lu, Appl. Catal. A 272 (2004) 329–338.
[21] P.E. Strizhak, A.I. Trypolskyi, G.R. Kosmambetova, O.Z. Didenko, T.N. Gurnyk, Kinet. Catal. 52 (2011) 128–138.
[22] G.C. Bond, Catal. Rev. 50 (2008) 532–567.
[23] G.C. Bond, Chem. Soc. Rev. 20 (1991) 441–475.
[24] G.C. Bond, Surf. Sci. 156 (1985) 966–981.